Universality in colloid aggregation

M. Y. Lin*¶, H. M. Lindsay†, D. A. Weitz*#, R. C. Ball‡, R. Klein§ & P. Meakin||

* Exxon Research and Engineering Co., Route 22E Annandale, New Jersey 08801, USA
† Physics Department, Emory University, Atlanta, Georgia 30322, USA
‡ The Cavendish Laboratory, Madingley Road, Cambridge CB3 9HE, UK
§ Facultät für Physik, Universität Konstanz, Konstanz, FRG
|| E. I. DuPont de Nemours Co., Experimental Station, Wilmington, Delaware 19880-0356, USA

THE aggregation of colloidal particles is of fundamental importance in colloid science and its applications. The recent application of scaling concepts[1,2] has resulted in a much deeper understanding of the structure of colloidal aggregates and the kinetics of their formation. Two distinct, limiting regimes of irreversible colloid aggregation have been identified[3]. Diffusion-limited colloid aggregation occurs when there is negligible repulsive force between the colloidal particles, so that the aggregation rate is limited solely by the time taken for clusters to encounter each other by diffusion. Reaction-limited colloid aggregation occurs when there is still a substantial, but not insurmountable, repulsive force beween the particles, so that the aggregation rate is limited by the time taken for two clusters to overcome this repulsive barrier by thermal activation. These regimes correspond to the limiting cases of rapid and slow colloid aggregation that have long been recognized in colloid science[4]. An intriguing possibility suggested by recent work is that each of these limiting regimes of colloid aggregation is universal, independent of the chemical details of the particular colloid system. Here we investigate the aggregation of three chemically different colloidal systems under both diffusion-limited and reaction-limited aggregation conditions. A scaling analysis of light-scattering data is used to compare the behaviour and provides convincing experimental evidence that the two regimes of aggregation are indeed universal.

The two regimes have been studied theoretically[5-8], by computer simulation[9-14] and by experimental studies of various colloids[3,15-21]. Each regime is distinguished by several distinct and characteristic features. The structures of the aggregates in both regimes are fractal, so that the mass (or number of particles in the cluster) scales as $M \propto (R_g/a)^{d_f}$, where R_g is the radius of gyration of the cluster and a is the radius of its constituent particles. The fractal dimension is $d_f \approx 1.8$ for diffusion-limited colloid aggregation (DLCA) and $d_f \approx 2.1$ for reaction-limited colloid aggregation (RLCA). For both regimes, the cluster mass distribution, $N(M)$, exhibits dynamic scaling, in that the shape becomes constant and universal in time. For DLCA, $N(M)$ is slightly peaked around the average cluster mass, $\bar{M}$, falling exponentially beyond it. For RLCA, on the other hand, the cluster mass distribution has a power-law form, again with an exponential cutoff, $N(M) \sim \bar{M}^{\tau-2} M^{-\tau} \exp(-M/\bar{M})$. In both cases, only $\bar{M}$ depends on time: for DLCA, $\bar{M}$ grows linearly in time, whereas for RLCA, $\bar{M}$ grows exponentially.

Here we investigate three very different colloids: colloidal gold, colloidal silica and polystyrene latex. The colloidal gold has primary particles with $a = 7.5$ nm and an initial volume fraction of $\phi_0 \approx 3 \times 10^{-6}$. The colloid is initially charge-stabilized by citrate ions adsorbed on the gold particle surfaces. Aggregation is initiated by the addition of pyridine, a neutral molecule which displaces the adsorbed citrate ions and thereby reduces the stabilizing charge. The aggregation rate is controlled by the amount of pyridine added: the final pyridine concentration is 10^{-2} M for DLCA and 10^{-4} M for RLCA. The interparticle bonds formed are probably metallic. The colloidal silica has $a = 3.5$ nm and is initially charge-stabilized by OH^- or SiO^- on the surface. Aggregation is induced by addition of NaCl, which decreases the Debye-Hückel screening length, thereby decreasing the repulsive barrier between the particles. For DLCA, $\phi_0 \approx 2 \times 10^{-6}$ and the salt concentration is 1.7 M; for RLCA, $\phi_0 \approx 1 \times 10^{-5}$ and the salt concentration is 0.6 M. The pH is maintained at ≥ 11 by addition of NaOH, which ensures that siloxane bonds are formed upon aggregation. The polystyrene latex has $a = 19$ nm and is initially charge-stabilized by adsorbed carboxylic acid groups. For DLCA, $\phi_0 \approx 8 \times 10^{-7}$ and HCl is added to a concentration of 1.2 M, both neutralizing the surface charge and decreasing the screening length. For RLCA, $\phi_0 \approx 7 \times 10^{-6}$ and NaCl is added to a concentration of 0.2 M, decreasing the screening length. The particle surfaces deform on bonding, leading to large van der Waals forces between the particles.

Graphic suggestion of the universal behaviour can be seen in the transmission electron micrographs shown in Fig. 1. Typical clusters formed in both the DCLA and RCLA regimes of aggregation are shown for each of the three colloids, and for computer-simulated clusters. The DLCA clusters are all more open and tenuous, reflecting their lower fractal dimension ($d_f < 2$), whereas the RLCA clusters are more compact, having $d_f > 2$. However, the similarity between the structures of the clusters within each regime is striking, suggesting a universal nature for the aggregation processes that lead to their formation.

To compare critically the behaviour of the colloids in each regime, we use static light scattering to measure the fractal

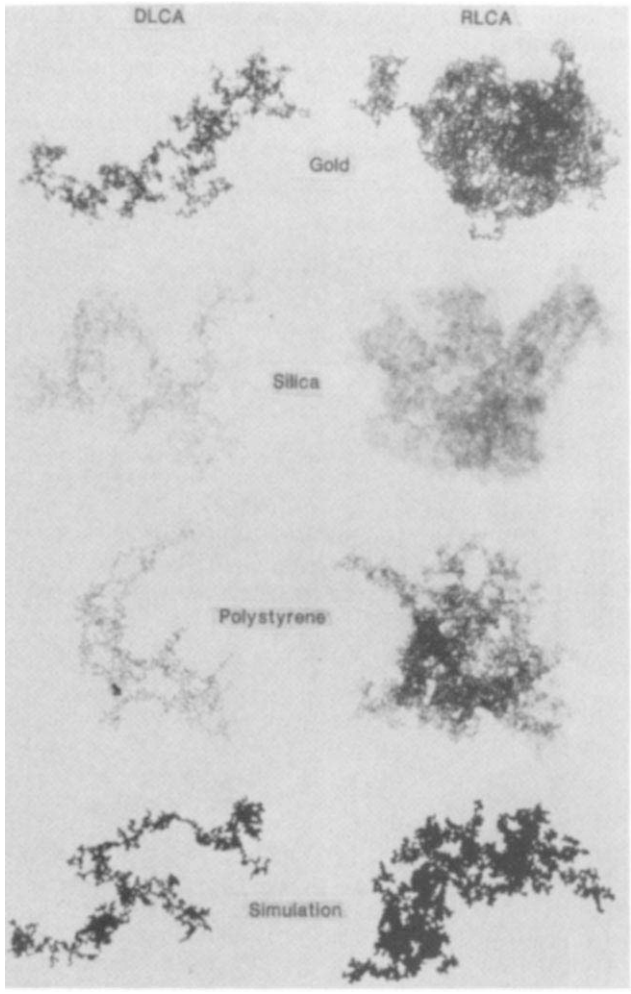

FIG. 1 Transmission electron micrographs of typical clusters of gold, silica and polystyrene colloids prepared by both diffusion-limited and reaction-limited cluster aggregation, and computer simulation. Note the striking similarity in the structure of the clusters of different colloids in each regime.

¶ Present address: Department of Physics, Princeton University, Princeton, New Jersey 08544, USA.
# To whom correspondence should be addressed.

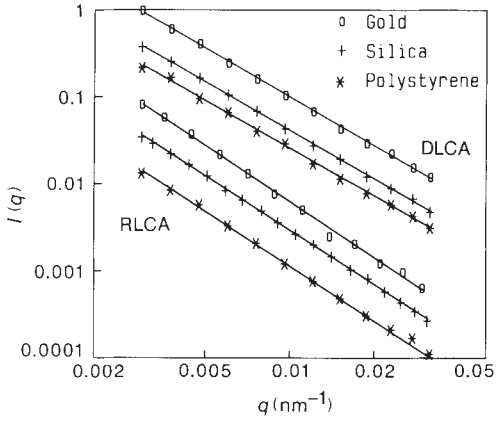

FIG. 2 Static light scattering measurements, showing universal behaviour in each regime. The linear behaviour of the data in the logarithmic plot is indicative of fractal clusters. For DLCA (top), the slopes give $d_f = 1.86$ for gold, $d_f = 1.85$ for silica and $d_f = 1.82$ for polystyrene. For RLCA (bottom) the slopes are consistently higher, with $d_f = 2.14$, 2.07 and 2.09, respectively.

structure of the aggregates, and quasielastic light scattering (QELS) to measure the aggregation kinetics and to probe the shape of the cluster mass distributions. We show that, for each regime, the QELS data can be scaled onto a single master curve, the shape of which depends on the key features of the aggregation process. Comparison of the shapes of the master curves for different colloids provides a critical test of the universality of the aggregation process in each regime.

The sensitivity of light scattering to the properties of colloidal aggregates arises from the dependence of the scattered intensity on the cluster size and the scattering vector, $q = (2\pi n/\lambda) \sin \theta/2$. Here $\lambda = 488$ nm is the wavelength of the laser light used, n is the index of refraction of the fluid and θ is the scattering angle. Because the fractal clusters are self-similar in structure, the scattered intensity is a function of the product qR_g. At low qR_g, the internal structure of the aggregate is not resolved, and the scattering is completely coherent, so that the intensity scales as M^2, independent of q. At high qR_g, however, the fractal structure of the cluster is resolved and the scattering intensity reflects this with a q^{-d_f} dependence. In this case the total intensity scales linearly with M.

Both static and dynamic light scattering average over the cluster mass distribution, $N(M)$. Static light scattering measures the time-averaged intensity, and hence is simply a sum over the distribution, weighted by the average scattering intensity for each cluster,

$$I(q) = \frac{\Sigma\, N(M) I(qR_g)}{\Sigma\, N(M) M} \qquad (1)$$

If $q\bar{R} \gg 1$, where $\bar{R}$ is the average cluster size, then $I(q) \propto q^{-d_f}$, directly reflecting the fractal dimension of the clusters. In Fig. 2, we show the static scattering from all the colloids, obtained with $q\bar{R} \gg 1$. For each regime, the slopes of the data are the same for each colloid, confirming the identical fractal structure of the aggregates, with $d_f = 1.85 \pm 0.1$ for DLCA and $d_f = 2.10 \pm 0.1$ for RLCA.

By contrast to the static light scattering, QELS measures the temporal fluctuations of the scattered intensity from the aggregates resulting from their diffusive motion. We measure the autocorrelation function of these fluctuations, and here restrict our attention to its initial logarithmic slope, or 'first cumulant', Γ_1. For a single cluster, $\Gamma_1 = q^2 D_{eff}(qR_g)$, where the effective diffusion coefficient D_{eff} reflects the contribution of both translational and rotational motion[22]. When $qR_g \ll 1$, only translational diffusion contributes and $D_{eff}(qR_g) = D = \zeta/R_H$, where $\zeta = kT/6\pi\eta$, and η is the fluid viscosity. The cluster's hydrodynamic radius R_H is proportional to its radius of gyration[23–25]: $R_H = \beta R_g$, where $\beta \approx 1$. However, at $qR_g \geq 1$, rotational diffusion also contributes to the intensity fluctuations, and $D_{eff}(R_g)$ increases towards a limiting value of $\sim 2D$. This qR_g dependence of D_{eff} reflects the anisotropy of the aggregates, giving QELS an additional sensitivity to the cluster structure.

The average D_{eff} measured by QELS is a sum over the distribution, weighted by the scattering intensity[22]:

$$\bar{D}_{eff} = \frac{\bar{\Gamma}_1}{q^2} = \frac{\Sigma\, N(M) I(qR_g) D_{eff}(qR_g)}{\Sigma\, N(M) I(qR_g)} \qquad (2)$$

This measures a different moment of the cluster mass distribution than does the static intensity. In the limit of $q \to 0$, $\bar{D}_{eff} = \bar{D}$, providing a good measure of the average cluster size, $\bar{R} = \zeta/\bar{D}$.

The combination of the sensitivity to the cluster mass distribution and to rotational diffusion leads to a pronounced q dependence in the measured $\bar{D}_{eff}$, and provides a very sensitive probe of the aggregation process. However, to fully explore this q dependence at a single point in time during the aggregation process would require an experimentally inaccessible range of scattering angles. Instead, we exploit the dynamic scaling of the cluster mass distribution to measure $\bar{D}_{eff}$ over a much wider range of $q\bar{R}$. Thus, we determine $\bar{D}_{eff}$ over the experimentally accessible range of q, and repeat the measurements during the aggregation process, as $\bar{R}$ increases while the shape of the cluster mass distribution remains unchanged. The values measured at each q are interpolated to obtain a series of data sets, each consisting of $\bar{D}_{eff}(q)$ evaluated at the same time. We normalize $\bar{D}_{eff}$ by $\bar{D}$, and plot the data as a function of $q\bar{R}$, where the required parameter, $\bar{D} = \zeta/\bar{R}$, for each set is determined empiri-

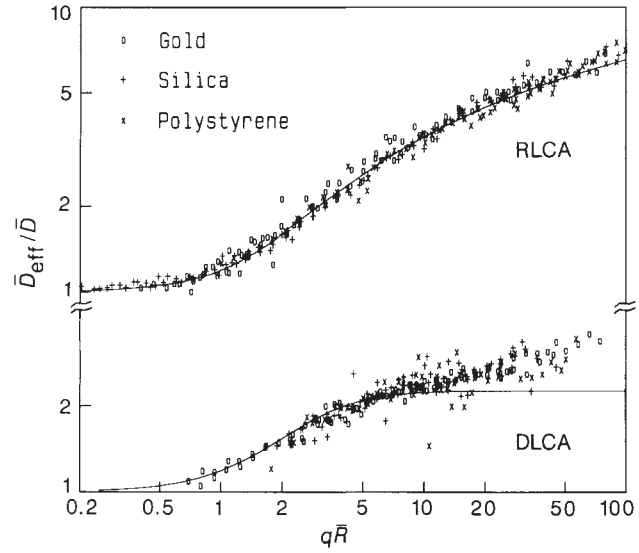

FIG. 3 Master curves from dynamic light scattering for each colloid for RLCA (top) and DLCA (bottom). All material parameters have been scaled out: the shape of the master curve is sensitive to the cluster mass distribution, the static scattering from the aggregates and the anisotropy in their structure. In each regime the master curves for different colloids are indistinguishable, showing the universality of colloid aggregation. The solid lines are theoretical calculations.

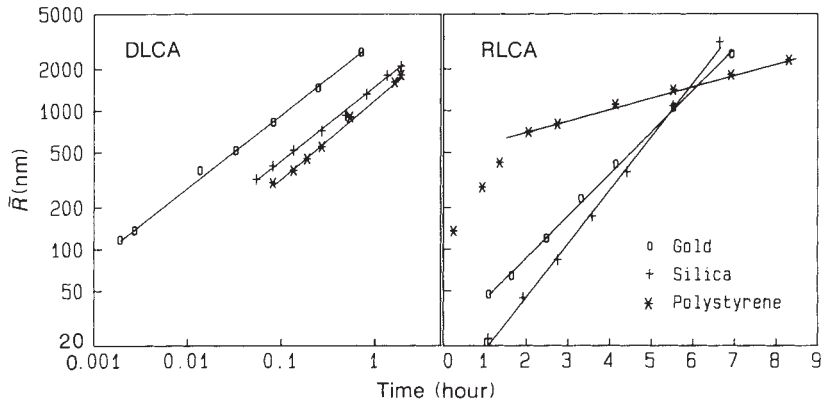

FIG. 4 Aggregation kinetics. For DLCA (left) the linear behaviour on the logarithmic plot indicates power-law kinetics, $\bar{R} \propto t^{\alpha}$. The fitted slopes give $\alpha = 0.53$ for gold, $\alpha = 0.54$ for silica and $\alpha = 0.56$ for polystyrene. For RLCA (right) the linear behaviour on the semi-logarithmic plot indicates exponential kinetics. The deviation from this behaviour for polystyrene is discussed in the text.

cally by scaling the data onto a single master curve. With sufficient data, there is always a substantial overlap between data from different sets, making the scaling unambiguous. All material parameters are scaled out, so that we obtain a critical comparison between the behaviour of completely different colloids.

The master curves obtained for each colloid in each regime are plotted in Fig. 3. The shape of the master curve for DLCA is different from that of RLCA, reflecting the different shapes of $N(M)$ for each regime; the power-law form for RLCA leads to a considerably stronger q dependence of the master curve. In each regime, the master curves for the three colloids are indistinguishable. We emphasize that the master curves for each colloid are obtained independently, and there is no free parameter in comparing them. This is striking evidence of the universality of each of the regimes of colloid aggregation.

We can also calculate[26] the shapes of the master curves for each regime using equation (2) and $I(qR_g)$ from simulation clusters. The results are shown by the solid lines in Fig. 3. For DLCA, we obtain good agreement with the data, except at high $q\bar{R}$. For RLCA, we obtain excellent agreement at all $q\bar{R}$, using an exponent for the cluster mass distribution of $\tau = 1.5$.

The scaling values of $\bar{R}$ accurately reflect the average cluster radius in the distribution at each time, and are therefore a useful measure of the aggregation kinetics, as shown in Fig. 4. The DLCA kinetics are power-law, $\bar{R} \propto t^{\alpha}$, for each colloid, showing linear behaviour on the logarithmic graph. The exponent is consistent with $\alpha = 1/d_f$, giving $\bar{M} \propto t$, as expected[7]. The different offsets of the curves reflect the different primary particle radii and different initial values of ϕ_0. By contrast, the RLCA kinetics are exponential, showing linear behaviour on the semi-logarithmic plot. Exponential kinetics are observed for the gold and the silica over all times, and for the polystyrene at later times.

The reaction-limited kinetics of polystyrene are initially exponential, then slow down dramatically (while still remaining exponential) after about one hour. This behaviour is observed for RLCA measurements using small polystyrene spheres, and is consistent with observations of others[27]. The absolute rate of aggregation, and the subsequent exponential kinetics, rule out the possibility of this representing a crossover to DLCA. As both the scaling of the master-curve data and the static scattering strongly indicate RLCA behaviour throughout, we suggest that this change results from an increase in the energy barrier between the particles at later times, associated with partial coalescence on aggregation, which has been observed for similar particles[28].

We have presented experimental evidence from three different colloid systems which demonstrates that the process of colloid aggregation is universal, independent of the detailed chemical nature of the colloids. This universality can be used to help rationalize deviations that are bound to occur (for example, the polystyrene RLCA kinetics). Biological molecules exhibit markedly different aggregation behaviour[27,29,30], producing clusters with considerably higher d_f. These observations may be understood if the clusters undergo considerable restructuring during aggregation.

We conclude by recalling that it has long been recognized that the stability of lyophobic colloids can be rationalized in universal terms by considering the interaction energy between two approaching particles. What is remarkable about the results presented here is that they demonstrate that the whole process of their aggregation is universal, thereby greatly extending our ability to understand the properties of colloids and their aggregates.

Note added in proof: A recent paper[31] has suggested that the aggregation behaviour of colloidal gold is different from that of other colloids, based on an interpretation of light-scattering data which is claimed to exhibit multiple scattering resulting from the optical resonance of the metallic particles. The results presented here demonstrate conclusively that both the static and dynamic light scattering from the gold aggregates is identical to that from the more weakly scattering dielectric aggregates, providing unambiguous evidence that there is no multiple scattering from the metallic clusters, and that the aggregation of colloidal gold is the same as the other colloids in each of the limiting, universal regimes. □

Received 16 February; accepted 17 April 1989.

1. Meakin, P. in *Phase Transitions* (ed. Liebowitz, J. L.) **12,** 335 (Academic, New York, 1988).
2. Jullien, R. & Botet, R. *Aggregation and Fractal Aggregates* (World Scientific, Singapore, 1987).
3. Weitz, D. A., Huang, J. S., Lin, M. Y. & Sung, J. *Phys. Rev. Lett.* **54,** 1416–1419 (1985).
4. Verwey, E. J. W. & Overbeek, J. T. G. *Theory of the Stability of Lyophobic Colloids* (Elsevier, Amsterdam, 1948).
5. Cohen, R. J. & Benedek, G. B. *J. phys. Chem.* **86,** 3696–3714 (1982).
6. Vicsek, T. & Family, F. *Phys. Rev. Lett.* **52,** 1669–1672 (1984).
7. Van Dongen, G. J. & Ernst, M. H. *Phys. Rev. Lett.* **54,** 1396–1399 (1985).
8. Ball, R. C., Weitz, D. A., Witten, T. A. & Leyvraz, F. *Phys. Rev. Lett.* **58,** 274–277 (1987).
9. Meakin, P. *Phys. Rev. Lett.* **51,** 1119–1122 (1983).
10. Kolb, M., Botet, R. & Jullien, R. *Phys. Rev. Lett.* **51,** 1123–1126 (1983).
11. Brown, W. D. & Ball, R. C. *J. Phys.* **A18,** L517–L519 (1985).
12. Mountain, R. D. & Mulholland, G. W. *Langmuir* **4,** 1321–1326 (1988).
13. Meakin, P., Vicsek, T. & Family, F. *Phys. Rev.* B**31,** 564–569 (1985).
14. Meakin, P. & Family, F. *Phys. Rev.* A**36,** 5498–5501 (1987).
15. Von Schultess, G. K., Benedek, G. B. & De Blois, R. W. *Macromolecules* **13,** 939–945 (1980).
16. Weitz, D. A. & Oliveria, M. *Phys. Rev. Lett.* **52,** 1433–1436 (1984).
17. Schaefer, D. W., Martin, J. E., Wiltzius, P. & Cannell, D. S. *Phys. Rev. Lett.* **52,** 2371–2374 (1984).
18. Matsushita, M., Hayakawa, Y., Sumida, K. & Sawada, Y. in *Science on Form: Proceedings of the First International Conference for Science on Form* (ed. Kato, Y., Takaki, R. & Toriwaki, J.) (KTK Scientific Publishers, Tokyo, 1986).
19. Aubert, C. & Cannell, D. S. *Phys. Rev. Lett.* **56** 738–741 (1986).
20. Weitz, D. A. & Lin, M. Y. *Phys. Rev. Lett.* **57,** 2037–2040 (1986).
21. Martin, J. E. *Phys. Rev.* A**36,** 3415–3426 (1987).
22. Lindsay, H. M., Klein, R., Weitz, D. A., Lin, M. Y. & Meakin, P. *Phys. Rev.* A**38,** 2614–2626 (1988).
23. Chen, Z.-Y., Deutch, J. M. & Meakin, P. *J. chem. Phys.* **80,** 2982–2983 (1984).
24. Hess, W., Frisch, H. L. & Klein, R. *Z. Phys.* B**64,** 65–68 (1986).
25. Wiltzius, P. *Phys. Rev. Lett.* **58,** 710–713 (1987).
26. Lin, M. Y. *et al. Proc. R. Soc. Lond.* A (in the press).
27. Rarity, J. G., Seabrook, R. N. & Carr, R. G., *Proc. Roy. Soc. Lond.* A (in the press).
28. Buscall, R., Mills, P. D. A., Goodwin, J. W. & Lawson, D. W. *J. chem. Soc. Faraday Trans.* **1,** 4249–4260 (1988).
29. Feder, J., Jossang, T. & Rosenqvist, E. *Phys. Rev. Lett.* **53,** 1403 (1984).
30. Horne, D. S. *Faraday Discuss. chem. Soc.* **83,** 259–270 (1987).
31. Wilcoxon, J. P., Martin, J. E. & Schaefer, D. W. *Phys. Rev.* A **39,** 2675–2688 (1989).

ACKNOWLEDGEMENTS. We thank John Dunsmuir and the two Deckmans for their help with the transmission electron micrographs.